

Mott transitions in ternary flavor mixtures of ultracold fermions on optical lattices

E. V. Gorelik and N. Blümer

Institute of Physics, Johannes Gutenberg University, 55099 Mainz, Germany

(Received 7 May 2009; revised manuscript received 9 July 2009; published 11 November 2009)

Ternary flavor mixtures of ultracold fermionic atoms in an optical lattice are studied in the case of equal repulsive on-site interactions $U > 0$. The corresponding SU(3) invariant Hubbard model is solved numerically exactly within dynamical mean-field theory using multigrid Hirsch-Fye quantum Monte Carlo simulations. We establish Mott transitions close to integer filling at low temperatures and show that the associated signatures in the compressibility and pair occupancy persist to high temperatures, i.e., they should be accessible to experiments. In addition, we present spectral functions and discuss the properties of a “semicompressible” state observed for large U near half filling.

DOI: [10.1103/PhysRevA.80.051602](https://doi.org/10.1103/PhysRevA.80.051602)

PACS number(s): 67.85.-d, 03.75.Ss, 71.10.Fd, 71.30.+h

Starting with the achievement of Bose-Einstein condensation in 1995, the creation and study of quantum degenerate atomic gases has led to discoveries with enormous impact far beyond atomic physics [1]. In particular, atomic gases can be driven to the strongly correlated regime by switching on optical lattices and/or using Feshbach resonances. In the bosonic case, the localized Mott phase is accessible already in single-component (lattice) systems [2]. With the recent observation [3,4] of Mott transitions in balanced two-flavor (i.e., two-hyperfine-state) mixtures of fermionic ^{40}K atoms with repulsive interactions, such systems are now established as highly tunable *quantum simulators* of condensed matter [5].

At the same time, ultracold atoms offer new degrees of freedom: in contrast to the electronic case, with only two spin states, fermionic atoms have large hyperfine multiplets. Early experiments [6] involving three hyperfine states of ^{40}K have prompted theoretical investigations of three-flavor mixtures on optical lattices. These studies have focused on the case of pairwise equal *attractive* interactions which may induce trionic phases and exotic superfluidity with a three-component order parameter, somewhat analogous to QCD [7]. Since 2008, balanced three-flavor ^6Li mixtures have been trapped and studied across Feshbach resonances [8,9]. Soon, such systems—both with repulsive and attractive interactions—should be realized also in optical lattices.

In this Rapid Communication, we explore the properties of fermionic three-flavor mixtures on optical lattices in the case of *repulsive* interactions. While the many ordering patterns conceivable in such systems will certainly warrant extensive studies at some point, ordering phenomena have escaped experimental detection even in the simpler two-flavor case so far. We will, thus, concentrate on the Mott physics of *homogeneous phases*. Note that this regime is particularly challenging since it requires nonperturbative theoretical approaches.

Ternary mixtures of fermions on an optical lattice can be modeled via the Hubbard-type Hamiltonian

$$\hat{H} = \sum_{\langle ij \rangle, \alpha} t_{\alpha} \hat{c}_{i\alpha}^{\dagger} \hat{c}_{j\alpha} + \sum_{i, \alpha < \alpha'} U_{\alpha\alpha'} \hat{n}_{i\alpha} \hat{n}_{i\alpha'} - \sum_{i, \alpha} \mu_{\alpha} \hat{n}_{i\alpha}. \quad (1)$$

Here, $\langle ij \rangle$ denotes nearest-neighbor sites, $\alpha \in \{1, 2, 3\}$ labels the fermionic flavors, t parametrizes the hopping, U is the

on-site Coulomb interaction, and μ is the chemical potential. In Eq. (1), we have neglected higher Bloch bands and the confining potential. For fermions of a single species (in the vibrational ground state), $t_{\alpha} \approx t_{\alpha'}$. Following the literature, we will also assume pairwise equal interactions and study the SU(3) symmetric limit $t_{\alpha} \equiv t$, $U_{\alpha\alpha'} \equiv U$, $\mu_{\alpha} \equiv \mu + U$; by this definition, particle-hole symmetry corresponds to a sign change in μ .

This system is treated within dynamical mean-field theory (DMFT), which retains the dynamics of local correlations [10]. The semielliptic “Bethe” density of states with bandwidth $W = 4t^*$ mimics [11] a simple cubic lattice (with $t = t^*/\sqrt{6}$); as usual in DMFT studies, the scale is set by the scaled hopping amplitude $t^* = \sqrt{Z}t$ for the coordination number Z . The DMFT impurity problem is solved using the Hirsch-Fye quantum Monte Carlo algorithm (HF-QMC) [12], first in the conventional form, with imaginary-time discretization $\Delta\tau \leq 0.8/U$; the validity of these results is later verified and unbiased results are obtained using the numerically exact multigrid implementation [13]. Note that already conventional HF-QMC is competitive with continuous-time QMC [14]; the multigrid variant is even more efficient. All QMC-based methods share the advantage, compared to numerical renormalization-group approaches, of being reliable at the experimentally relevant (elevated) temperatures.

Results at low temperature. Theoretical studies of electronic one-band models are often restricted to half filling ($\mu = 0$). Mott metal-insulator transitions are, then, signaled by kinks or jumps in thermodynamic properties (as a function of interaction U and/or temperature T) or, more directly, by the opening of a gap in the local spectral function $A(\omega)$. In the present three-flavor case, genuine Mott physics can be expected only far away from particle-hole symmetry; consequently, the chemical potential μ is an essential additional parameter. In the following, we will choose a relatively low temperature $T = t^*/20$ and explore the (U, μ) space with particular emphasis on properties that are most accessible in quantum gas experiments and which are related to Mott physics. Temperature effects and spectral functions are to be discussed later.

Figure 1 shows the filling $n = \sum_{\alpha} \langle \hat{n}_{\alpha} \rangle$ versus the chemical potential μ for a range of on-site interactions U . Initially, for $U = 0$, n varies smoothly and rapidly with μ from an empty

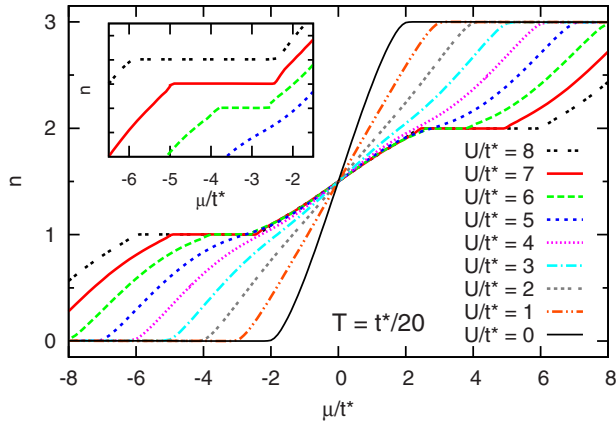


FIG. 1. (Color online) HF-QMC estimates of particle density $n(\mu)$ at $T=t^*/20$ for various on-site interactions U . Plateaus at integer filling indicate localized Mott phases (for $U/t^* \geq 6$). In the inset, curves are shifted (in steps of 0.1) for clarity.

band ($n=0$) at $\mu/t^* \leq -2$ to a full band ($n=3$) at $\mu/t^* \geq 2$. With increasing U , the slope generally decreases, but the curves remain smooth until, for $U/t^* \geq 6$, plateaus develop at integer fillings $n=1, n=2$, which signal the onset of localized Mott phases (and correspond to gaps in the spectral function). The particle-hole symmetry around $\mu=0$ is evident; from now on, we will only consider $\mu \leq 0$. The plateaus appear perfectly flat even at the magnified scale of the inset of Fig. 1 (for $n=1$); tendencies toward hysteresis are seen for $U/t^*=6$ (at $\mu/t^* \approx -2.5$). We will argue below that $T=t^*/20$ is very close to the critical temperature T^* of a second-order Mott critical end point (cf. Fig. 4).

From our results, detailed predictions for experimental measurements can be derived within the local-density approximation (LDA). For a specific trap potential and atom number, the data of Fig. 1 then translate to occupancies n_i of the inhomogeneous system, integrated column densities, and cloud sizes. Analogous approaches have been used in the Bloch-Rosch collaboration for establishing the Mott phase in the two-flavor case [4,15].

A fundamental property of Mott phases is the suppression of density fluctuations; in the two-flavor case these are usually quantified by the double occupancy $\langle \hat{n}_i \hat{n}_{i\downarrow} \rangle$. In the present three-flavor context, we consider the more general pair occupancy $D = \sum_{\alpha < \alpha'} \langle \hat{n}_{i\alpha} \hat{n}_{i\alpha'} \rangle$, which retains the energy relation $E = E_{\text{kin}} + UD$ [16]. As seen in the main panel of Fig. 2, D depends strongly on μ and U ; the dependence on μ is mostly monotonic, except for the vicinity of plateaus (for $U/t^* \geq 6$). The impact of U is best understood at fixed density n (see inset of Fig. 2): starting from the noninteracting limit $U=0$, where $D=n^2/3$, D is suppressed with increasing U at all n . This suppression is strongly enhanced at $n=1$ for $U/t^* \geq 6$. Fortunately, the probabilities for n -fold occupancy can be easily measured experimentally. In fact, this technique has been used by the Esslinger group for detecting Mott phases in the two-flavor case via changes in the slopes dD/dn close to integer filling [3]; analogous slopes are marked by thick line segments in the inset of Fig. 2.

One interesting feature of Fig. 1 not discussed so far is that the slopes $dn/d\mu$ seem to saturate in the range

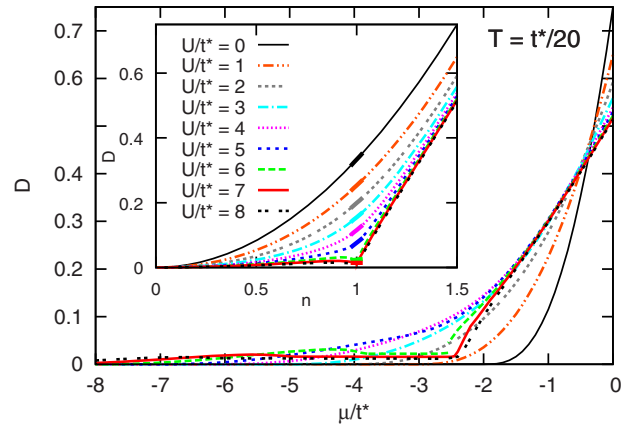


FIG. 2. (Color online) HF-QMC estimates of pair occupancy D at $T=t^*/20$ vs chemical potential μ (main panel) and vs density n (inset), respectively. The suppression of D with increasing U is clearly enhanced on the Mott plateau at $n \approx 1$.

$-2 \leq \mu/t^* \leq 2$ for large U . The corresponding compressibility $\kappa = dn/d\mu$ [17], computed via numerical differentiation of the data of Fig. 1, is shown in Fig. 3. Note that—in contrast to expressions such as $n^{-1}dn/d\mu$ —this definition of κ retains the particle-hole symmetry [$\kappa(-\mu) = \kappa(\mu)$] and fulfills a sum rule [$\int_{-\infty}^{\infty} \kappa(\mu) d\mu = 3$], just as the spectral function. Indeed, $\kappa(\mu)$ reduces to the slightly broadened semielliptic spectral function for $U=0$ (thick solid line in Fig. 3). With increasing U , the height of this central peak is rapidly reduced and the weight of $\kappa(\mu)$ is shifted toward larger $|\mu|$, with a subpeak at $|\mu| \approx U+t^*$ developing for $U/t^* \geq 2$. The intermediate minima are initially smooth; their positions coincide with integer filling as is apparent from the curves $\kappa(n)$ shown in the inset of Fig. 3. Finally, for $U/t^* \geq 6$, sharp gaps appear; these Mott plateaus [$\kappa(\mu) \approx 0$] collapse to points in the representation $\kappa(n)$.

Coming back to the saturation of slopes $dn/d\mu$, let us first note that the peak value $\kappa(\mu=0)$ reaches a finite limit of about $0.2/t^*$ for large U (and low T), i.e., scales with the inverse of the (only remaining) energy scale $W \propto t^*$. Even more importantly, the variation in $\kappa(\mu)$ within the central

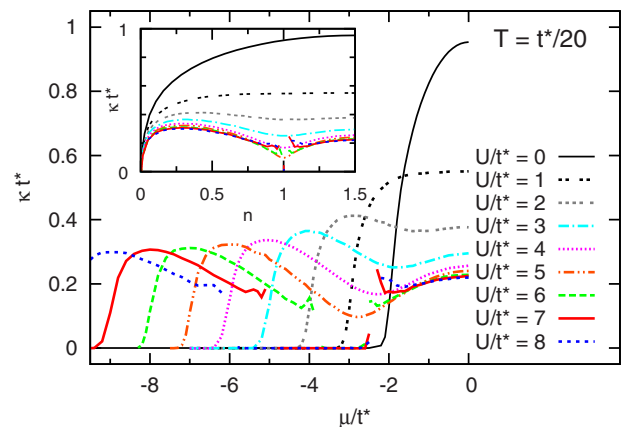


FIG. 3. (Color online) HF-QMC estimates of compressibility $\kappa = dn/d\mu$ at $T=t^*/20$ as a function of chemical potential μ (main panel) and density n (inset), respectively.

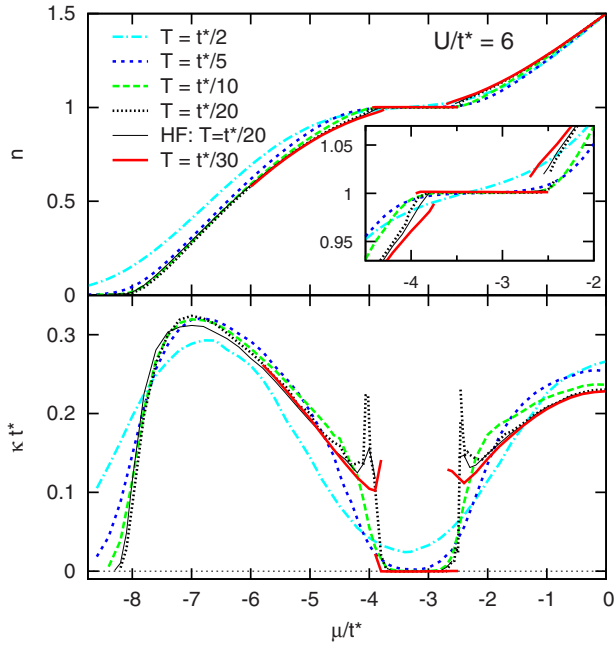


FIG. 4. (Color online) Multigrad HF-QMC estimates of density $n(\mu)$ (top panel) and compressibility $\kappa(\mu) = dn(\mu)/d\mu$ (bottom panel) at interaction $U/t^* = 6$ for various temperatures T . The strong suppression of κ at $n \approx 1$ survives up to $T \approx t^*/5 \gg T^* \approx t^*/20$. For comparison, thin solid lines indicate HF-QMC data for $T = t^*/20$ (cf. Figs. 1 and 3).

compressible phase decreases with increasing U until κ is nearly constant for $U/t^* \geq 8$ [in contrast with the edge phase ($n < 1$) where κt^* varies between 0 and about 0.3]. This additional plateau marks a semicompressible state sandwiched between two equivalent Mott phases, which is specific to $SU(2M+1)$ systems ($M \geq 1$) [18] and should be easy to probe experimentally.

Impact of temperature. While experiments with fermionic atomic gases in optical lattices offer much greater flexibility in varying interaction and hopping parameters (compared to solid-state experiments), they are currently restricted by initial temperatures not much lower than the Fermi temperature T_F . On the other hand, true Mott transitions and/or ordering phenomena typically occur on energy scales that are one to two orders of magnitude below the kinetic-energy scales (such as T_F or the bandwidth W). Therefore, it is essential to study the systems of interest also at elevated temperatures and, if possible, to identify signatures of Mott transitions which persist to temperatures much higher than the critical temperatures, i.e., signal well-defined crossover regions. At the same time, good estimates of the critical temperature(s) T^* of the Mott transitions are desirable.

In Fig. 4, we present multigrad HF-QMC estimates (thick lines) of $n(\mu)$ (top panel) and $\kappa(\mu)$ (bottom panel) for a wide range of temperatures at a relatively strong interaction $U/t^* = 6$. Clearly, the temperature effects are small across wide regions of μ , with deviations in n typically on the order of 10^{-2} for $T \leq t^*/5$. However, extended hysteresis regions at the plateau edges are observed only at the lowest temperature, $T = t^*/30$. At $T = t^*/20$, coexistence is hardly significant (around $\mu/t^* \approx -2.5$) while the compressibility is strongly

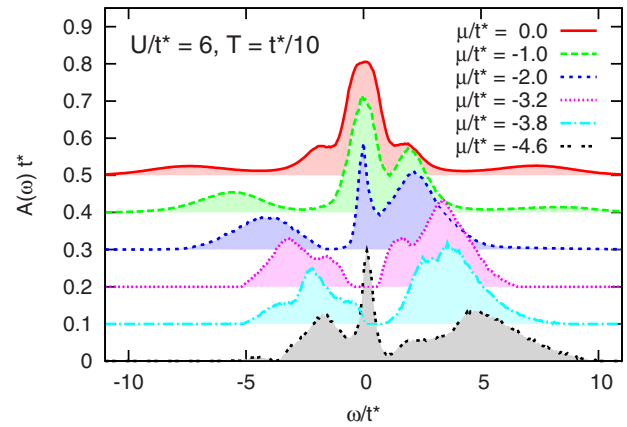


FIG. 5. (Color online) Multigrad HF-QMC estimates of spectral function $A(\omega)$ for $T = t^*/10$, $U/t^* = 6$ at different values of μ , corresponding to densities $n = 1.5, 1.27, 1.07, 1.00, 0.9996$, and 0.91 (from top to bottom).

enhanced in both transition regions, as expected very close to second-order critical end points [17]. Consequently, we estimate the critical temperature as $T^* = (0.05 \pm 0.01)t^*$. At higher temperatures, all curves are smooth. Nevertheless, a Mott plateau can be identified up to $T = t^*/5$: in the central region $\mu/t^* \approx -3.3$, the compressibility is still reduced by two orders of magnitude compared to off-plateau regions. This is good news for experimentalists: a factor of 4 above the critical temperature [roughly corresponding to an entropy $s = \ln(3)$ per particle], the (remnant of the) Mott plateau should still be well visible. Even at $T = t^*/2$, a full order of magnitude above T^* , the compressibility is more strongly reduced, in the Mott crossover region, than at the subcritical interaction $U/t^* = 5$ for low T (cf. Fig. 3). A similar picture emerges for the pair occupancy (not shown): both the plateaus and the nonmonotonic behavior in $D(\mu)$ persist up to $T \leq t^*/5$.

Also shown in Fig. 4 are conventional HF-QMC estimates for $T = t^*/20$ (and $\Delta\pi^* = 0.12$; thin solid lines). The good agreement with the numerically exact multigrad HF-QMC Green's functions for $U/t^* = 6$. At half filling (top curve), $A(\omega)$ is symmetric and shows a rough three-peak structure (with peaks at $\omega = 0$ and $\omega/t^* \approx \pm 7$), reminiscent of the familiar one-band-two-spin correlated metallic phase. However, important differences arise in the three-flavor case: (i) the Hubbard bands, although well separated, carry little weight (of about 10% each); (ii) the central peak (at $|\omega/t^*| \leq 4$) has a threefold substructure; and (iii) the quasiparticle peak remains for arbitrary U (with only 10% reduction in weight for $5 \leq U/t^* \leq 10$; not shown).

Spectra. Finally, let us discuss an experimentally more challenging observable: the local spectral function $A(\omega)$. Figure 5 shows estimates obtained via maximum entropy analytic continuation from numerically exact multigrad HF-QMC Green's functions for $U/t^* = 6$. At half filling (top curve), $A(\omega)$ is symmetric and shows a rough three-peak structure (with peaks at $\omega = 0$ and $\omega/t^* \approx \pm 7$), reminiscent of the familiar one-band-two-spin correlated metallic phase. However, important differences arise in the three-flavor case: (i) the Hubbard bands, although well separated, carry little weight (of about 10% each); (ii) the central peak (at $|\omega/t^*| \leq 4$) has a threefold substructure; and (iii) the quasiparticle peak remains for arbitrary U (with only 10% reduction in weight for $5 \leq U/t^* \leq 10$; not shown).

With decreasing filling, triply occupied sites become even less important: the upper Hubbard band vanishes for $\mu/t^* \leq -2$. In contrast, the lower band rapidly acquires

weight: about 26% for $\mu/t^*=-1$, while the quasiparticle peak shrinks at nearly constant peak height [$A(0)t^*\approx 0.3$]. It disappears when μ reaches the Mott plateau, at $\mu/t^*=-3.2$, a well-defined central gap has opened. The remaining peaks have centers of mass at $\omega=-2.8t^*$ and $\omega=3.2t^*$, respectively; the difference exactly equals the interaction U , just as one would expect in the half-filled two-spin case. However, in the present three-flavor case (also at $n=1$), the weights are strongly asymmetric: $1/3$ and $2/3$ for the lower and upper Hubbard bands (of which the latter has formed from the central peak at $n=1.5$), respectively. For further decreased μ , a quasiparticle peak reappears from the lower subband.

In this nonperturbative study of the repulsive SU(3) symmetric Hubbard model, we have thoroughly explored its homogeneous phases at low and intermediate temperatures in the (U, μ) space. We have shown that signatures of Mott transitions close to integer filling persist to elevated temperatures, facilitating the experimental observation of strong correlation phenomena, e.g., in balanced three-flavor mixtures of ^{40}K (with roughly equal positive scattering lengths at small magnetic fields [6]) or ^6Li [8,9] on optical lattices;

systems with Raman excited states [19] provide an interesting alternative.

We have found peculiar features in spectra and a semi-compressible phase with asymptotically universal κ (independent of U , T , and μ or n), which is clearly linked with the presence of adjacent *equivalent* Mott lobes. Experimental studies of this physics might be challenging, but are within reach of existing techniques.

Our work could be extended toward full quantitative correspondence with upcoming experiments by explicit inclusion of the trap potential, within LDA (similar to recent studies [4,20,21] for two-flavor systems) or beyond [15,22]; also, ordered phases [22,23] could be considered. It seems, however, more urgent to investigate which properties of SU(3) symmetric systems survive for unequal interactions (with less severe three-body losses [8,9]), when flavor-selective Mott physics [24] may be expected.

We thank I. Bloch, P. G. J. van Dongen, W. Hofstetter, Á. Rapp, and U. Schneider for discussions. Support by the DFG within the TR 49 and by the John von Neumann Institute for Computing is gratefully acknowledged.

-
- [1] I. Bloch, J. Dalibard, and W. Zwerger, *Rev. Mod. Phys.* **80**, 885 (2008).
- [2] M. Greiner, O. Mandel, T. Esslinger, T. W. Hänsch, and I. Bloch, *Nature (London)* **415**, 39 (2002).
- [3] R. Jördens, N. Strohmaier, K. Günter, H. Moritz, and T. Esslinger, *Nature (London)* **455**, 204 (2008).
- [4] U. Schneider *et al.*, *Science* **322**, 1520 (2008).
- [5] I. Bloch, *Science* **319**, 1202 (2008).
- [6] C. A. Regal and D. S. Jin, *Phys. Rev. Lett.* **90**, 230404 (2003).
- [7] C. Honerkamp and W. Hofstetter, *Phys. Rev. B* **70**, 094521 (2004); Á. Rapp, G. Zaránd, C. Honerkamp, and W. Hofstetter, *Phys. Rev. Lett.* **98**, 160405 (2007); Á. Rapp, W. Hofstetter, and G. Zaránd, *Phys. Rev. B* **77**, 144520 (2008); F. Wilczek, *Nat. Phys.* **3**, 375 (2007).
- [8] T. B. Ottenstein, T. Lompe, M. Kohnen, A. N. Wenz, and S. Jochim, *Phys. Rev. Lett.* **101**, 203202 (2008).
- [9] J. H. Huckans, J. R. Williams, E. L. Hazlett, R. W. Stites, and K. M. O'Hara, *Phys. Rev. Lett.* **102**, 165302 (2009).
- [10] G. Kotliar and D. Vollhardt, *Phys. Today* **57**(3), 53 (2004).
- [11] In the filling range $0.7\leq n\leq 2.3$, this approximation shifts static properties at most by a few percent.
- [12] J. E. Hirsch and R. M. Fye, *Phys. Rev. Lett.* **56**, 2521 (1986).
- [13] N. Blümer, e-print arXiv:0801.1222.
- [14] N. Blümer, *Phys. Rev. B* **76**, 205120 (2007).
- [15] R. W. Helmes, T. A. Costi, and A. Rosch, *Phys. Rev. Lett.* **100**, 056403 (2008).
- [16] The probability of double (but not triple) occupancy is $\tilde{D}\equiv D-3\langle n_{i_1}n_{i_2}n_{i_3}\rangle$; however, for $\mu\leq 0$, $D\approx\tilde{D}$.
- [17] G. Kotliar, S. Murthy, and M. J. Rozenberg, *Phys. Rev. Lett.* **89**, 046401 (2002).
- [18] In SU($2M$) systems ($M\geq 2$), metallic phases can only be sandwiched between inequivalent Mott phases, which appears to induce strong variations in $dn/d\mu$; S. Florens and A. Georges, *Phys. Rev. B* **70**, 035114 (2004).
- [19] T. Müller, S. Fölling, A. Widera, and I. Bloch, *Phys. Rev. Lett.* **99**, 200405 (2007).
- [20] L. De Leo, C. Kollath, A. Georges, M. Ferrero, and O. Parcollet, *Phys. Rev. Lett.* **101**, 210403 (2008).
- [21] V. W. Scarola, L. Pollet, J. Oitmaa, and M. Troyer, *Phys. Rev. Lett.* **102**, 135302 (2009).
- [22] M. Snoek, I. Titvinidze, C. Töke, K. Byczuk, and W. Hofstetter, *New J. Phys.* **10**, 093008 (2008).
- [23] C. Honerkamp and W. Hofstetter, *Phys. Rev. Lett.* **92**, 170403 (2004).
- [24] See, e.g., C. Knecht, N. Blümer, and P. G. J. van Dongen, *Phys. Rev. B* **72**, 081103(R) (2005).